Phys. Status Solidi B **249**, No. 2, 270–275 (2012) / **DOI** 10.1002/pssb.201100530

physica status solidi b
www.pss-b.com
basic solid state physics

Feature Article

First-principles Liouville–von Neumann equation for open systems and its applications

Siu Kong Koo[1], Chi Yung Yam*[,1], Xiao Zheng[2], and GuanHua Chen[1]

[1] Department of Chemistry, The University of Hong Kong, Pokfulam Road, Hong Kong
[2] Hefei National Laboratory for Physical Sciences at Microscale, University of Science and Technology of China, Hefei, P.R. China

Received 1 September 2011, revised 8 November 2011, accepted 8 November 2011
Published online 23 December 2011

Dedicated to Thomas Frauenheim on the occasion of his 60th birthday

Keywords density functional theory, Liouville–von Neumann equation, open system, quantum transport, time-dependent DFT

* Corresponding author: e-mail yamcy@yangtze.hku.hk, Phone: (+852) 2859 8045, Fax: (+852) 2915 5176

We present a first-principles Liouville–von Neumann equation for open systems. The time-dependent holographic electron density theorem which is the foundation for our formalism is introduced. Approximation schemes for practical simulations are given. In order to demonstrate the applicability of our formalism, a realistic simulation of a simple molecular device system is presented and discussed.

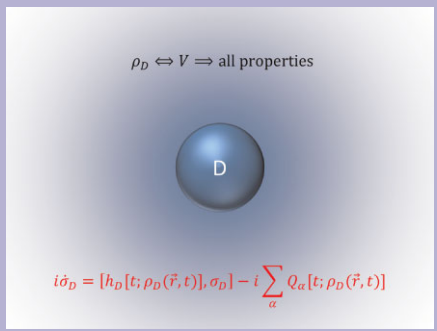

1 Introduction In the last decades, the size of electronic circuits reduced continuously. Following the International Technology Roadmap for Semiconductors, the miniaturization of the devices found in integrated circuits is predicted to reach atomic dimensions in few years' time. Today, the ultimate limit of miniaturization has already been achieved in laboratory that current across single molecules between metallic leads could be successfully measured [1, 2]. In such case, quantum mechanical treatments are crucial in order to capture the atomistic details and quantum effects in such a small device properly. Much theoretical and experimental research efforts have been put into the aspect of the quantum transport through nanostructures [3–15].

The combined density functional theory (DFT) and non-equilibrium Green's function (NEGF) approach enjoy popularity in the context of quantum transport, which reduces to the traditional Landauer–Büttiker formalism for coherent transport. The majority of such studies for realistic devices focus on steady state currents under bias voltages. Recently, time-dependent density functional theory (TDDFT) has also been developed to study quantum transport phenomena [5, 7–13]. As a formally exact and numerically tractable approach, TDDFT not only provides a more rigorous theoretical foundation, but also allows for the description of dynamical processes like the switching behavior of electronic devices and time-dependent currents. In this paper, we present the resulting first-principles Liouville–von Neumann equation based on TDDFT for open systems and a practical computational scheme to provide a comprehensive theoretical tool for studying nanoscale electronics devices.

This paper is organized as follows. In Section 2, basics of density functional theory and density functional theory for open system, i.e., the Hohenberg–Kohn theorem and holographic electron density theorem, is briefly introduced. The first-principles Liouville–von Neumann equation for open systems is also presented which governs the time

propagation of the reduced single-electron density matrix. To demonstrate the applicability of our first-principle formalism, we have performed simulations on a molecular device system. The detailed numerical procedures and results are shown in Section 3, followed by a summary in Section 4.

2 Methodology The Hohenberg–Kohn (HK) theorem [16] states that the ground state electron density function determines all electronic properties of the system. Based on this theorem, a practical scheme was formulated by Kohn and Sham [17] in order to calculate the ground-state properties of electronic systems. As an extension of the HK theorem, the Runge–Gross theorem [18] states that the time-dependent electron density function determines uniquely all electronic properties of the corresponding time-dependent system. The Runge–Gross theorem provides the foundation for development of time-dependent density-functional theory (TDDFT) for calculating excited-state properties of electronic systems.

Analogously, holographic electron density theorems (HEDT) lay the foundations for DFT and TDDFT for open systems. Fournais et al. [19, 20] have proved in 2004 that electron density function of any time-independent real physical systems made of atoms and molecules is real analytic except at nuclei. In 2010, Jecko has given a simpler proof for the real analyticity of electron density [21]. This real analyticity of electron density provides a solid basis for the ground-state holographic electron density theorem (GS-HEDT) which states that any nonzero volume piece of the ground-state electron density determines the electron density of the entire system [22, 23]. The GS-HEDT was extended to time-dependent systems and the time-dependent holographic electron density theorem (TD-HEDT) states that if the electron density function of a real finite physical system at t_0, $\rho(\vec{r}, t_0)$, is real analytic in $\vec{r}$-space, the corresponding wave function is $\Phi(t_0)$, and a real analytic (in both t-space and $\vec{r}$-space) external potential field $v(\vec{r}, t)$ is applied to the system after t_0, the time-dependent electron density function on any finite subspace D, $\rho_D(\vec{r}, t)$, has a one-to-one correspondence with $v(\vec{r}, t)$ (up to an additive merely time-dependent function), and determines all electronic properties of the entire time-dependent system uniquely. TD-HEDT proves the existence of TDDFT for open systems, and a detailed proof of TD-HEDT can be found in Ref. [24].

On the basis of the existence of an exact TDDFT for open systems, we have developed a practical first-principles approach to simulate transient electrical response of molecular devices [9, 12]. Our TDDFT formalism for open system starts from a closed equation of motion (EOM) for the Kohn–Sham (KS) reduced single-electron density matrix (RSDM) of the entire system, $\sigma(t)$:

$$i\dot{\sigma}(t) = [h(t), \sigma(t)], \tag{1}$$

where $h(t)$ is the KS Fock matrix. Equation (1) is the Liouville–von Neumann equation which governs the time evolution of $\sigma(t)$. We can easily see that with a simple coordinate transformation and a Fourier transformation, the Wigner distribution function form of the Liouville–von Neumann equation can be recovered from Eq. (1) [25]. A simple open system is illustrated in Fig. 1 schematically, which a molecular device is coupled with two electrodes being connected to an external bias. By using atomic orbital basis sets, σ can be expanded and partitioned as

$$\sigma = \begin{bmatrix} \sigma_L & \sigma_{LD} & \sigma_{LR} \\ \sigma_{DL} & \sigma_D & \sigma_{DR} \\ \sigma_{RL} & \sigma_{RD} & \sigma_R \end{bmatrix}, \tag{2}$$

where σ_L, σ_D, and σ_R are the diagonal blocks corresponding to the left lead L, the device region D, and the right lead R, respectively. The off-diagonal block between L and D is denoted as σ_{LD}; and similarly, σ_{DL}, σ_{RD}, σ_{DR}, σ_{LR}, σ_{RL} are defined in the same manner. The KS Fock matrix can also be partitioned into the same pattern. Hence, we can get the EOM for σ_D:

$$i\dot{\sigma}_D = [h_D, \sigma_D] - i \sum_{\alpha=L,R} Q_\alpha, \tag{3}$$

and

$$Q_\alpha = i(h_{D\alpha}\sigma_{\alpha D} - \sigma_{D\alpha}h_{D\alpha}), \tag{4}$$

where Q_L and Q_R are the dissipative terms due to L and R, respectively. According to the TD-HEDT, Q_α is in principle a functional of electron density in the sub-system D, $\rho_D(\vec{r}, t)$, and therefore Eq. (4) can be recast into a formally closed form

$$i\dot{\sigma}_D = [h_D[t; \rho_D(\vec{r}, t)], \sigma_D] - i \sum_{\alpha=L,R} Q_\alpha[t; \rho_D(\vec{r}, t)]. \tag{5}$$

Equation (5) is the first-principles Liouville–von Neumann equation for quantum open systems and the transient electric current though the interface S_α can be evaluated through

$$I_\alpha(t) = -\int_\alpha d\vec{r} \frac{\partial}{\partial t} \rho(\vec{r}, t) = -\mathrm{tr}[Q_\alpha(t)]. \tag{6}$$

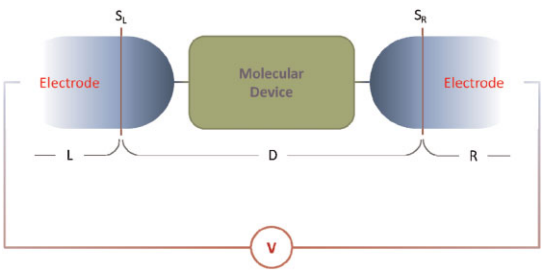

Figure 1 (online color at: www.pss-b.com) Schematic representation of a simple experimental setup for quantum transport through a molecular device. L, D, and R denote the left electrode region, device region, and right electrode region, respectively. L and R are connected to an external bias. S_L(S_R) represents the interface between D and L(R). Adequate portion of the electrodes are included into D, so that S_L(S_R) will show bulk properties of L(R).

In practice, conventional local or semilocal density approximation for XC potential can be adopted to construct the KS Fock matrix $h_{\rm D}[t;\rho_{\rm D}(\vec{r},t)]$. The challenge here is to express $Q_\alpha[t;\rho_{\rm D}(\vec{r},t)]$ in a formally exact and numerically accessible way [26]. Based on the Keldysh formalism, we have

$$Q_{\alpha,\mu\nu}(t) = -\sum_{l\in{\rm D}} \int_{-\infty}^{+\infty} {\rm d}\tau \Big[G^<_{\mu l}(t,\tau)\Sigma^{\rm a}_{\alpha,l\nu}(\tau,t) + G^{\rm r}_{\mu l}(t,\tau)\Sigma^<_{\alpha,l\nu}(\tau,t)\Big] + {\rm H.c.}], \tag{7}$$

where $G^<$ and $G^{\rm a}$ are the lesser and advanced Green's functions respectively, and $\Sigma^<$ and $\Sigma^{\rm a}$ are the lesser and advanced self-energies, respectively. Practically, we consider an approximate scheme for $Q_\alpha(t)$ based on a wide-band limit (WBL) treatment for electrodes, as well as an adiabatic approximation for memory effect. The scheme aims at simplifying the NEGF expression of $Q_\alpha(t)$ [9],

$$Q^{\rm AWBL}_\alpha(t) = \{\Lambda_\alpha, \sigma_{\rm D}\} + P_\alpha(t) + [P_\alpha(t)]^\dagger. \tag{8}$$

Here, $P_\alpha(t)$ can be evaluated by

$$P_\alpha(t) \approx -\frac{i}{\pi}\Bigg\{ U_\alpha(t)\int_{-\infty}^{+\infty} {\rm d}\varepsilon f_\alpha(\varepsilon){\rm e}^{i\varepsilon t} \times \left[\frac{1}{\varepsilon - h_{\rm D}(0) + i\Lambda} - \frac{1}{\varepsilon - h_{\rm D}(t) + i\Lambda + \Delta_\alpha(t)}\right] + \int_{-\infty}^{+\infty} \frac{f_\alpha(\varepsilon)}{\varepsilon - h_{\rm D}(t) + i\Lambda + \Delta_\alpha(t)}{\rm d}\varepsilon\Bigg\}\Lambda_\alpha, \tag{9}$$

and

$$U_\alpha(t) \equiv {\rm e}^{-i\int_0^t {\rm d}\tau[h_{\rm D}(\tau) - i\Lambda - \Delta_\alpha(\tau)]}, \tag{10}$$

where $f_\alpha(\varepsilon)$ is the Fermi distribution function for the electrode α. $\Delta_\alpha(t)$ is the energy shift for all single-electron levels in electrode α due to the time-dependent applied voltage. $\Lambda = \Lambda_{\rm L} + \Lambda_{\rm R}$ gives the device-electrode coupling matrix.

Alternatively, a hierarchical equation of motion (HEOM) [12, 26] is developed where for non-interacting systems, such as TDKS reference system in the present case, the hierarchy terminates exactly at the second tier without any approximation [26]. Within the TDDFT-NEGF-HEOM formalism, the Liouville–von Neumann equation reads

$$i\dot{\sigma}_{\rm D} = [h_{\rm D}, \sigma_{\rm D}] - \sum_\alpha [\varphi_\alpha(t) - \varphi^\dagger_\alpha(t)], \tag{11}$$

where φ is the first-tier auxiliary RSDM and is directly associated with the dissipation functional Q_α as follows:

$$Q_\alpha(t) = -i\big[\varphi_\alpha(t) - \varphi^\dagger_\alpha(t)\big] = -i\int {\rm d}\varepsilon\big[\varphi_\alpha(\varepsilon,t) - \varphi^\dagger_\alpha(\varepsilon,t)\big]. \tag{12}$$

The corresponding HEOM for the KS RSDM and its auxiliary counterparts have been derived in Ref. [26] as follows:

$$i\dot{\varphi}_\alpha(\varepsilon,t) = [h_{\rm D}(t) - \varepsilon - \Delta_\alpha(t)]\varphi_\alpha(\varepsilon,t) + [f_\alpha(\varepsilon) - \sigma_{\rm D}]\Lambda_\alpha(\varepsilon) + \sum_{\alpha'}\int {\rm d}\varepsilon'\varphi_{\alpha,\alpha'}(\varepsilon,\varepsilon',t) \tag{13}$$

and

$$i\dot{\varphi}_{\alpha,\alpha'}(\varepsilon,\varepsilon',t) = -[\varepsilon + \Delta_\alpha(t) - \varepsilon' - \Delta_{\alpha'}(t)]\varphi_{\alpha,\alpha'}(\varepsilon,\varepsilon',t) + \Lambda_{\alpha'}(\varepsilon')\varphi_\alpha(\varepsilon,t) - \varphi^\dagger_{\alpha'}(\varepsilon',t)\Lambda_\alpha(\varepsilon). \tag{14}$$

In practice, quadrature rules such as Gauss–Legendre quadrature may be used for the frequency integration.

3 Results and discussion We have carried out numerical simulations using our formalism. We have employed the adiabatic local-density approximation (ALDA) for the exchange-correlation (XC) potential, and AWBL approximation for the dissipation functional. We used the in-house built software package, LODESTAR [27–30], to perform the calculations.

The system of interest is a model molecular device. A benzene ring is sandwiched between two linear carbon chains which serve as electrodes, see Fig. 2. We have included explicitly in the simulation box sixteen carbon atoms and four hydrogen atoms. The ground-state KS Fock matrix of the extended system which includes extra portions of electrodes of fifteen carbon atoms on each side is calculated self-consistently with LDA. Linear carbon chain is a relatively good electric conductor, so the induced electrostatic potential by external voltage is assumed to be constant for the bulk electrode far away from the device. The boundary condition for solving Poisson equation for Hartree potential inside the simulation box in our calculation is given by a rigid shift of the KS potential of the electrodes. The same procedure has been widely adopted in quantum transport simulations [11, 31]. The minimal basis set STO-3G is adopted in the calculations. For the propagation, the fourth-order Runge-Kutta method is employed to integrate Eq. (5) in the time domain.

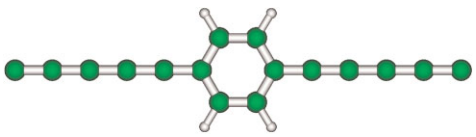

Figure 2 (online color at: www.pss-b.com) The ball and stick representation of a model molecular device system, a C–benzene–C system. A benzene ring is sandwiched between two infinitely long linear carbon chains which serve as the electrodes. Only the device region is shown in this figure. The green balls are carbon atoms while the white balls are hydrogen atoms.

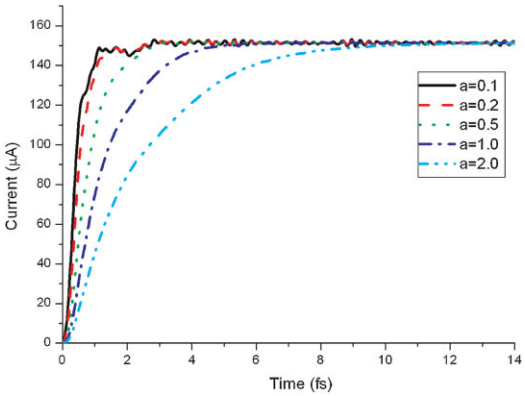

Figure 3 (online color at: www.pss-b.com) Transient currents for our C–benzene–C system. The bias voltage is switched on exponentially, $V(t) = V_0(1 - e^{-t/a})$ with $V_0 = 3$ V and time constant $a = 0.1$, 0.2, 0.5, 1.0, and 2.0 fs, respectively. The currents through the system with the applied bias voltages having different a are represented by different line types.

The bias voltage is turned on exponentially at $t = 0$ with a time constant a, according to $V(t) = V_0(1 - e^{-t/a})$. Figure 3 depicts the transient currents for the benzene molecule at different values of a with $V_0 = 3$ V. Although the establishments of the steady state follow different traces in different cases, they all reach to the same final steady state current. We have also applied a sinusoidal bias voltage across the system with a period of 2 fs. The time-dependent voltage and the corresponding electric current response are plotted in Fig. 4. The current from left electrode and that from right electrode are the same, in other words, the magnitude of the current entering and leaving the system are the same. The transient current obtained from Eq. (6) contains contribution from particle current only. Since the system has central inversion symmetry, there should be minimal charge accumulation or depletion in the system. The contribution from displacement current is thus negligible. The current establishes starting from the first cycle, and soon after that, the current reaches its quasi-steady state at the second cycle. Upon the quasi-steady state, it is observed that there is a constant phase difference between the bias voltage and the current response. From the figure, we can estimate that the bias voltage is ahead of the current by about 50.4°. This indicates that the system is overall inductive.

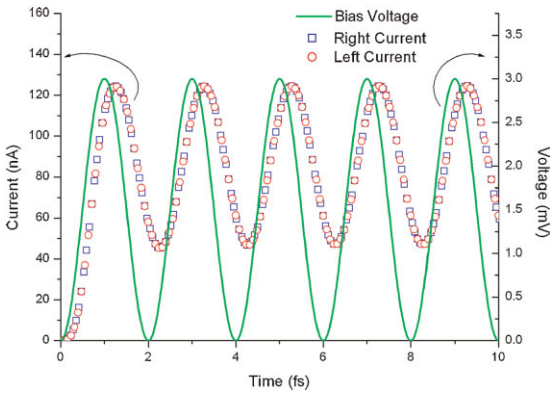

Figure 4 (online color at: www.pss-b.com) Transient current (open circles and squares) and applied bias voltage (solid line) for the C–benzene–C system. The bias voltage is sinusoidal with a period of 2 fs. The open circles are representing current from the left electrode, while the open squares are representing that from the right electrode.

Figure 5a depicts the dynamic admittance of the C–benzene–C system in linear regime. Due to symmetry, the admittance element $G_{\alpha\beta}(\omega)$ (for α, $\beta = $ L, R) satisfies $G_{LL} = -G_{LR} = -G_{RL} = G_{RR} = G(\omega)$ [32–34]. The dynamic admittance is obtained by $G(\omega) = I(\omega)/V(\omega)$, where $I(\omega)$ and $V(\omega)$ are obtained by Fourier transformation of $I(t)$ and $V(t)$, respectively. In the linear response regime, the dynamic admittance of a system should remain the same regardless of the type of bias voltage. This is confirmed by our numerical results. As shown in Fig. 5a, the system gives the same dynamic admittance for both exponential and sinusoidal time-dependent applied bias voltage. The response in nonlinear regime is more complex, and the discussion on model system has been covered elsewhere [35].

According to the above results and analysis, and our previous work [35–37], our system can be modeled by a simple classical circuit, with a resistor and an inductor connecting in series, in parallel with a resistor and a capacitor

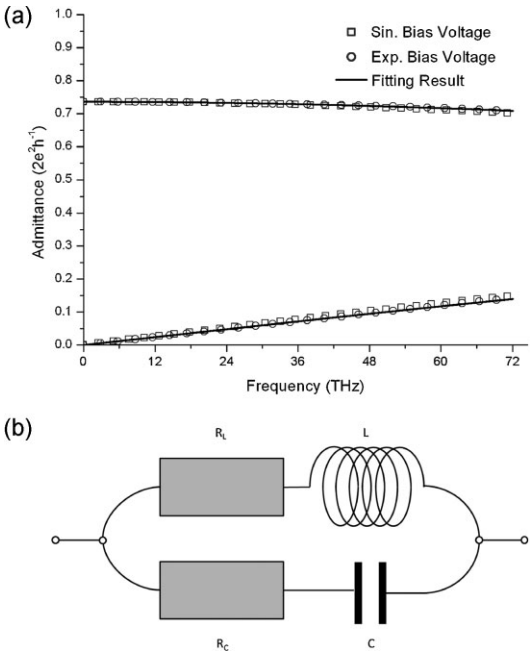

Figure 5 (a) Dynamic admittance of the C–benzene–C system. The data calculated with an exponential bias voltage, $V(t) = V_0(1 - e^{-t})$ and a sinusoidal bias voltage, $V(t) = V_0/2[1 - \cos(\pi t)]$ are represented by open circles and open squares, respectively. The solid lines show the result fitted by the classical equivalent circuit. The upper curves and the lower curves are the real and imaginary part of the admittance, respectively. (b) The equivalent classical electric circuit of our system. The fitted values of L, R_L, C, and R_C are 7.56 pH, 17.5 kΩ, 0.509 zF, and 12.9 kΩ, respectively.

connecting in series, see Fig. 5b. R_L is the steady state resistance, which is calculated to be 17.5 kΩ. The charge relaxation resistance $R_C = h/2e^2$ is independent of transmission details [38]. The dynamic admittance of a R–L R–C circuit under an AC bias voltage of frequency ω can be expressed as $G(\omega) = 1/(R_C + 1/i\omega C)^{-1} + (R_L + i\omega L)^{-1}$. Based on this expression, we can calculate the value of L by fitting the calculated dynamic admittance. The resulting values of L and C are 7.56 pH and 0.509 zF, respectively. The kinetic inductance L is proportional to the dwell time, τ_d, of electrons inside the device, $L \sim \tau_d h/e^2$ where $\tau_d \sim l/v_F$ with l being the length of the device and v_F being the Fermi velocity of the electrons [39]. The C–benzene–C system form a π-conjugate system across the whole device and the charge accumulation at the interfaces is thus small, leading to a very small C value. From the results, the studied system has very small value of L and C, hence the switching time of this nanoscale device is ultra-short.

The steady state obtained from our Liouville–von Neumann equation is compared with the conventional DFT-NEGF approach. The asymptotic values of the transient currents are extracted and compared to the static DFT results using the same WBL approximation for the leads. Figure 6a shows the I–V characteristics of the system in linear response regime with covered bias voltage ranging from 0 to 1 mV. It is clearly shown that the steady state current from both approaches yields identical results. This supports the earlier analytical arguments on the equivalence of static and dynamic local DFT approaches in linear response regime [40, 41]. Figure 6b shows the I–V curves of another set of simulations that the covered bias voltage was extended to 5 V in which the bias window contains one or more of the energy levels. Clearly, the WBL approximation breaks down in this situation, but the comparison of static and dynamic calculations is still meaningful since they are performed under exactly the same boundary conditions. The results in Fig. 6b show clearly that the static DFT-NEGF calculation yields the same results as the TDDFT approach over the whole bias range including the region of resonant transmission. This confirms our recent results on carbon chain and benzenediol systems [42].

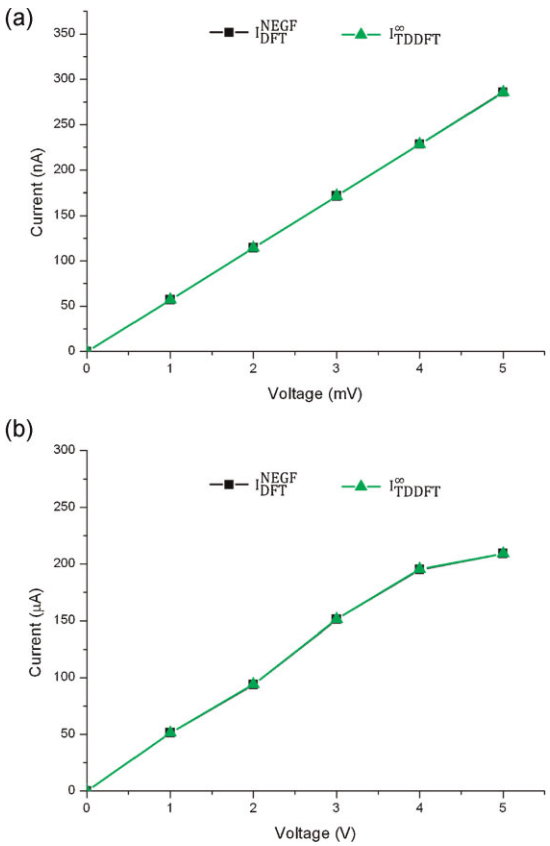

Figure 6 (online color at: www.pss-b.com) I–V curves of the C–benzene–C system at (a) low bias and (b) high bias regime. The results of TDDFT calculations are represented by the green lines and the static DFT-NEGF results by are represented by the black lines.

Quantum transport has also been studied using Liouville–von Neumann equation with Markovian approximation [43–45] and periodic boundary conditions [45]. While these methods apply to simple models, such as double barrier model structures or effective mass model, we presents in this work a first-principles Liouville–von Neumann equation for realistic systems with the use of AWBL approximation. In addition, the TDDFT-NEGF-HEOM has been developed which goes beyond the AWBL approximation and is in principle rigorous within the Runge–Gross formalism.

4 Summary The first-principles Liouville–von Neumann equation for open systems is presented, which includes all electrons and full atomistic details for both the electrodes and the nanoscopic device. We have also provided a numerical tractable approximation scheme for our formalism so that realistic simulation can be carried out. In order to show the applicability, we have performed simulations on a model two-terminal molecular device using our formalism. Transient currents through the device with different applied voltages were calculated. Dynamic electric response was investigated. For this system, we found that such dynamic response can be precisely mapped onto a very simple equivalent classical circuit, which agrees with our early finding on equivalent electric circuit [36, 37]. We have also compared the results from time dependent calculations and that from static calculations, and we have confirmed the consistency between these two kinds of calculations.

Our formalism gives a comprehensive approach for theoretical study of nanoelectronic devices, detailed temporal evolution and spatial distribution of the system can be obtained. This provides important guidelines for designing of emerging electronics in future.

Acknowledgements We thank the Hong Kong University Grant Council (AoE/P-04/08), Hong Kong Research Grant Council (HKU700909P, HKUST9/CRF/08, HKU700808P, and HKU701307P) and The University of Hong Kong (UDF on Fast

Algorithm Seed Funding Programme for Basic Research 2010-11159085 and 201010159001) for the support.

References

[1] M. A. Reed, C. Zhou, C. J. Muller, T. P. Burgin, and J. M. Tour, Science **278**, 252 (1997).
[2] S. J. Tans, M. H. Devoret, H. Dai, A. Thess, R. E. Smalley, L. J. Geerligs, and C. Dekker, Nature **386**, 474 (1997).
[3] J. Gabelli, G. Fève, J-M. Berroir, B. Placais, A. Cavanna, B. Etienne, Y. Jin, and D. C. Glattli, Science **313**, 499 (2006).
[4] A. Prêtre, H. Thomas, and M. Büttiker, Phys. Rev. B **54**, 8130 (1996).
[5] J. Maciejko, J. Wang, and H. Guo, Phys. Rev. B **74**, 085324 (2006).
[6] M. A. Topinka, B. J. LeRoy, S. E. J. Shaw, E. J. Heller, R. M. Westervelt, K. D. Maranowski, and A. C. Gossard, Science **289**, 2323 (2000).
[7] S. H. Ke, R. Liu, W. T. Yang, and H. U. Baranger, J. Chem. Phys. **132**, 234105 (2010).
[8] X. Zheng and G.H. Chen, arXiv:physics 0502021.
[9] X. Zheng, F. Wang, C. Y. Yam, Y. Mo, and G. H. Chen, Phys. Rev. B **75**, 195127 (2007).
[10] G. Stefanucci and C-O. Almbladh, Europhys. Lett. **67**, 14 (2004).
G. Stefanucci and C. O. Almbladh, Phys. Rev. B **69**, 195318 (2004).
G. Stefanucci, E. Perfetto, and M. Cini, Phys. Rev. B **81**, 115446 (2010).
[11] S. Kurth, G. Stefanucci, C.-O. Almbladh, A. Rubio, and E. K. U. Gross, Phys. Rev. B **72**, 035308 (2005).
[12] X. Zheng, G. H. Chen, Y. Mo, S. K. Koo, H. Tian, C. Y. Yam, and Y. J. Yan, J. Chem. Phys. **133**, 114101 (2010).
[13] J. Yuen-Zhou, D. G. Tempel, C. A. Rodríguez-Rosario, and A. Aspuru-Guzik, Phys. Rev. Lett. **104**, 043001 (2010).
[14] D. G. Tempel, M. A. Watson, R. Olivares-Amaya, and A. Aspuru-Guzik, arXiv:10040189v2.
[15] P. Myöhänen, A. Stan, G. Stefanucci, and R. van Leeuwen, Phys. Rev. B **80**, 115107 (2009).
[16] P. Hohenberg and W. Kohn, Phys. Rev. **136**, B864 (1964).
[17] W. Kohn and L. J. Sham, Phys. Rev. **140**, A1133 (1965).
[18] E. Runge and E. K. U. Gross, Phys. Rev. Lett. **52**, 997 (1984).
[19] S. Fournais, M. Hoffmann-Ostenhof, T. Hoffmann-Ostenhof, and T. O. Sorensen, Commun. Math. Phys. **228**, 401 (2002).
[20] S. Fournais, M. Hoffmann-Ostenhof, T. Hoffmann-Ostenhof, and T. O. Sorensen, Ark. Mat. **42**, 87 (2004).
[21] T. Jecko, Lett. Math. Phys. **93**, 73 (2010).
[22] J. Riess and W. Münch, Theor. Chim. Acta **58**, 295 (1981).
[23] P. G. Mezey, Mol. Phys. **96**, 169 (1999).
[24] X. Zheng, C. Y. Yam, F. Wang, and G. H. Chen, Phys. Chem. Chem. Phys. **13**, 14358 (2011).
[25] W. R. Frensley, Rev. Mod. Phys. **62**, 745 (1990).
G. H. Chen and S. Mukamel, J. Chem. Phys. **103**, 9355 (1995).
[26] J. S. Jin, X. Zheng, and Y. J. Yan, J. Chem. Phys. **128**, 234703 (2008).
[27] S. Yokojima and G. H. Chen, Chem. Phys. Lett. **292**, 379 (1998).
S. Yokojima and G. H. Chen, Phys. Rev. B **59**, 7259(1999).
[28] C. Y. Yam, S. Yokojima, and G. H. Chen, J. Chem. Phys. **119**, 8794 (2003).
C. Y. Yam, S. Yokojima, and G. H. Chen, Phys. Rev. B **68**, 153105 (2003).
F. Wang, C. Y. Yam, and G. H. Chen, J. Chem. Phys. **126**, 134104 (2007).
[29] G. H. Chen, C. Y. Yam, S. Yokojima, W. Z. Liang, X. J. Wang, F. Wang, and X. Zheng, http://yangtze.hku.hk/LODESTAR/lodestar.php.
[30] W. Z. Liang, S. Yokojima, and G. H. Chen, J. Chem. Phys. **110**, 1844 (1999).
W. Z. Liang, S. Yokojima, D. H. Zhou, and G. H. Chen, J. Phys. Chem. A **104**, 2445 (2000).
W. Z. Liang, X. J. Wang, S. Yokojima, and G. H. Chen, J. Am. Chem. Soc. **122**, 11129 (2000).
W. Z. Liang, S. Yokojima, M. F. Ng, G. H. Chen, and G. He, J. Am. Chem. Soc. **123**, 9830 (2001).
[31] A.-P. Jauho, N. S. Wingreen, and Y. Meir, Phys. Rev. B **50**, 5528 (1994).
[32] B. Wang, J. Wang, and H. Guo, Phys. Rev. Lett. **82**, 398 (1999).
[33] Y. Fu and S. C. Dudley, Phys. Rev. Lett. **70**, 65 (1993).
Y. Fu and S. C. Dudley, Phys. Rev. Lett. **71**, 466 (1993).
[34] R. Landauer, IBM J. Res. Dev. **1**, 223 (1975).
R. Landauer, Philos. Mag. **21**, 863 (1970).
[35] Y. Mo, X. Zheng, G. H. Chen, and Y. J. Yan, J. Phys.: Condens. Matter **21**, 355301 (2009).
[36] S. Z. Wen, S. K. Koo, C. Y. Yam, X. Zheng, Y. J. Yan, Z. M. Su, K. N. Fan, L. Cao, W. P. Wang, and G. H. Chen, J. Phys. Chem. B **115**, 5519 (2011).
[37] C. Y. Yam, Y. Mo, F. Wang, X. B. Li, G. H. Chen, X. Zheng, Y. Matsuda, J. Kheli-Tahir, and W. A. Goddard, III Nanotechnology **19**, 495203 (2008).
[38] M. Büttiker, A. Prêtre, and H. Thomas, Phys. Rev. Lett. **70**, 4114 (1993).
M. Büttiker, A. Prêtre, and H. Thomas, Phys. Rev. Lett. **71**, 465 (1993).
[39] J. Wang, B. G. Wang, and H. Guo, Phys. Rev. B **75**, 155336 (2007).
[40] F. Evers, F. Weigend, and M. Koentopp, Phys. Rev. B **69**, 235411 (2004).
N. Sai, M. Zwolak, G. Vignale, and M. Di Ventra, Phys. Rev. Lett. **94**, 186810 (2005).
G. Vignale and M. Di Ventra, Phys. Rev. B **79**, 014201 (2009).
[41] G. Stefanucci, S. Kurth, E. K. U. Gross, and A. Rubio, Theor. Comput. Chem. **17**, 247 (2007).
[42] C. Y. Yam, X. Zheng, G. H. Chen, Y. Wang, Th. Frauenheim, and T. A. Niehaus, Phys. Rev. B **83**, 245448 (2011).
[43] F. Rossi, A. Di Carlo, and P. Lugli, Phys. Rev. Lett. **80**, 3348 (1998).
[44] R. C. Iotti, E. Ciancio, and F. Rossi, Phys. Rev. B **72**, 125347 (2005).
[45] R. Gebauer and R. Car, Phys. Rev. B **70**, 125324 (2004).